

Power Systems Performance under 5G Radio Access Network in a Co-Simulation Environment

Rahul Iyer^{1*}, Biplav Choudhury^{2*}, Vijay K. Shah² and Ali Mehrizi-Sani¹

¹Power and Energy Center, ²Wireless@Virginia Tech

Bradley Department of Electrical and Computer Engineering, Virginia Tech, Blacksburg, VA. USA

Emails:{irahulrajan, biplavc, vijays, mehrizi}@vt.edu

Abstract—Communication can improve control of important system parameters by allowing different grid components to communicate their states with each other. This information exchange requires a reliable and fast communication infrastructure. 5G communication can be a viable means to achieve this objective. This paper investigates the performance of several smart grid applications under a 5G radio access network. Different scenarios including set point changes and transients are evaluated, and the results indicate that the system maintains stability when a 5G network is used to communicate system states.

Index Terms—5G, distributed control, resource allocation, scheduling, smart grids.

I. INTRODUCTION

5G is the most recent wireless communication standard that improves rates and reliability over older generations such as 4G/LTE. Prominent applications of 5G communications include remote mining, vehicular communications, healthcare, and military [1]. All these applications rely on the extremely high data rates and reliability supported by 5G. In general, 5G applications are categorized into three main types based on their performance requirements: (i) *enhanced mobile broadband (eMBB)*: eMBB involves providing 5G connectivity to traditional cellphones which is expected to be its most commonly used application, (ii) *ultra reliable low latency communications (URLLC)*: URLLC is designed for critical applications where reliability is extremely important, e.g., driving or robotic surgery, and (iii) *massive machine type communications (mMTC)*: mMTC is designed for massive internet of things (IoT) devices where battery performance is more important than data rates.

5G also has applications in control of the modern power system, often referred to as the smart grid. Smart grid leverages communication techniques to collect and distribute information about the system measurements to various grid components and the control center. For example, real-time feedback on electricity consumption can be used to dynamically adjust energy generation with the objective of improving energy

efficiency [2]. Traditionally, communication in power grid is designed using optical fibers which can be expensive as the grid becomes larger due to the large-scale connectivity needed between all the components involved [3]. Therefore, there is a timely opportunity for a use case for providing connectivity to power grid components through 5G. Third-generation partnership project (3GPP) recently formed a study group to standardize the end-to-end architecture of 5G networks specifically built for aiding smart grid operations and is expected to be formalized by Release 18 [4].

There has been a recent focus on investigating the benefits that connectivity can bring in smart grids. The authors in [5] compare the response of a fault management system 4G-LTE and 5G systems. The results indicate that machine-to-machine connectivity abilities of 5G provide significant performance improvement compared with 4G. Reference [6] reviews several applications that 5G can enable in smart grids and analyzes the associated challenges. In [7], a network servicing both eMBB and URLLC applications is considered, and its ability in handling line protection through URLLC is analyzed. The results show that provided the network coverage is above a certain threshold, differential line protection can be supported by the network. However, these research studies consider only a black box view of the 5G network without considering the implications of its various subsystems on the overall performance. This paper tries to address this gap.

This paper implements a co-simulation environment for power system and communication networks and employs this in an example application for distributed control. Distributed control techniques in smart grids involve distributed energy resources (DER) that coordinate for higher reliability and performance [8], especially where centralized control is impractical. This can happen due to a large number of DERs, privacy and security requirements, and computational implications. Distributed control can be applied at different levels, including primary [9] and secondary [10].

The contributions of this work are

- A Python-based 5G radio access network (RAN) simulator is developed to interface with general purpose power systems simulators such as PSCAD and MATLAB, thereby creating a co-simulation environment where the power grid components can communicate with each other through 5G links. This allows us to simulate the effects of RAN resource allocation on the smart grid. The RAN simulator is robust in terms of both interfacing with

* Both first authors contributed equally to this work.

This work is supported in part by the National Science Foundation under awards ECCS-1953198 and ECCS-1953213 and in part by the Commonwealth Cyber Initiative, an investment in the advancement of cyber R&D, innovation, and workforce development (www.cyberinitiative.org).

This paper has been accepted for publication in IEEE ISIE 2021. This is a preprint version of the accepted paper.

the different software environments and the number of devices that communicate within the power system.

- The suitability of 5G in supporting the specific use cases of a power park and coordinated set point modulation is investigated using this co-simulation environment.
- The performance of the smart grid under a 5G network is compared with an ideal scenario where the power grid components can communicate instantaneously.

The rest of the paper is organized as follows: Section II describes the overall design of the co-simulator and the interactions between the power and communication systems. Section III describes the 5G communication simulator in more detail. Sections IV and V present two power system use cases and show their performance in the presence of a 5G RAN. Finally, Section VI concludes the paper.

II. CO-SIMULATOR DESIGN

The objective of developing the co-simulation environment is to investigate the performance of a smart grid in the presence of a 5G RAN. The power system scenarios are simulated in software tools PSCAD and MATLAB, and the communication environment is implemented through a Python script.

The Python script models the 5G communication between the smart grid DERs. Consider the scenario shown in Fig. 1. The DERs generate packets containing their state information, i.e., their local measurements, which need to be transmitted to the other DERs depending on the application. This transmission can be done when the DERs are allocated resources by the 5G Base Station (gNodeB), where these resources are the means to support the communication links. In 5G, these resources are termed resource blocks (RB) and RBs are allocated based on the number of packets a DER wants to transmit, which is known as that DER's buffer status report (BSR). Co-simulation operates as described below:

- Each DER transmits its BSR status to the Python-based gNodeB at an interval of τ . This allows gNodeB to get the buffer status, i.e., packets pending to be sent from each DER.
- Based on BSR, gNodeB allocates RBs to DERs using a pre-defined resource allocation policy π at each transmission time interval (TTI). Based on the allocated RBs, DERs are allowed to transmit their information, i.e., pass their values to the Python simulator. This information exchange between PSCAD and Python script is done through writing the values to a text file.
- At each TTI, time is synchronized between the communication and power systems by allowing both of them to simultaneously step through the same duration of time.

The general design of the co-simulator is shown in Fig. 2. More details are discussed in Section III.

III. COMMUNICATION SYSTEM DESIGN

A round-robin policy π is used in our case where equal number of RBs are granted to each DER in a circular fashion, i.e., RBs are allocated to each DER in turn. Additionally, each DER transmits channel state information reference signal (CSI-RS) to gNodeB which is an indicator of channel quality.

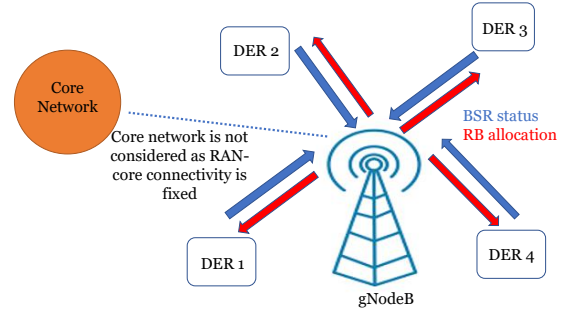


Fig. 1. Schematic diagram of a 5G Radio Access Network

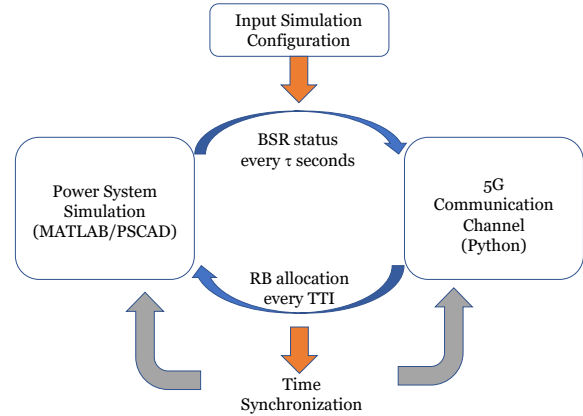


Fig. 2. Design of the proposed co-simulator.

This indicator is called channel quality index (CQI) and provides information about the modulation order that can be used, where modulation order is the number of symbols that can be transmitted. Better CQI allows the use of higher modulation order. The channel is modeled as a random time-varying channel which results in varying modulation orders over the allocated RBs, where higher modulation order means higher throughput. M RBs are considered and based on the RB allocation, the throughput achieved in Mbps in each of the communication link is calculated as per 3GPP TS 38.306 [11]. This is shown in (1).

$$10^{-6} \sum_{j=1}^J (v_{\text{Layers}}^{(j)} Q_m^{(j)} f^{(j)} R_{\text{max}} \frac{12 N_{\text{PRB}}^{BW(j),\mu}}{T_s^\mu} (1 - OH^j)) \quad (1)$$

Here J is the number of carriers aggregated in a carrier aggregation scenario. In 5G, up to 16 carriers can be aggregated. v_{Layers}^j is the maximum number of layers in the j th component carriers (CC). It is also the number of streams and is restricted by the number of antennas used. $Q_m^{(j)}$ defines the modulation order used which depends on CQI. $f^{(j)}$ is the scaling factor used to scale throughput for various CC combinations. R_{max} is the maximum coding rate and is typically set to $\frac{948}{1024}$ [12]. $N_{\text{PRB}}^{BW(j),\mu}$ is the number of RBs allocated to a single DER. μ defines the 5G numerology selected, and this numerology decides the symbol time, T_s^μ , calculated as $T_s^\mu = \frac{10}{14.2^\mu}$.

Finally, the overhead $OH(j)$ for carrier j is decided by the frequency band used (FR1 or FR2). gNodeB and DERs communicate in the FR1 band [13] (410 MHz to 7.125 GHz) using a bandwidth of B . Bandwidth is the range of radio wave frequencies allocated from the FR1 band. This achieved throughput decides the instants of information receptions at the DERs. Simulation parameters are shown in Table I.

The BSR and CQI reports are assumed to be sent out of band (without the need of resources for transmission) and are assured error-free reception at the gNodeB [14]. Therefore the gNodeB always knows the BSR and CQI at each TTI. The 5G RAN is connected to a core network (CN). As CN is a fiber cable-based network, the delay and reliability of this RAN-CN connection is fixed and do not vary [7]. Therefore, we do not model the CN and instead focus on the RB allocation in the RAN network. As a result, the network performance is investigated from the perspective of RB allocation.

TABLE I
PARAMETERS USED TO SET UP THE SIMULATION

Parameter	Value
Aggregated carriers J	2
Modulation order $Q_m^{(j)}$	2, 4, 6, 8
Maximum layers for j th carrier $v_{Layers}^{(j)}$	2
Scaling factor $f^{(j)}$	0.8
Numerology μ	2
Number of RBs M	3
RBs allocated per DER $N_{PRB}^{BW(j)}$	1
Scheduling policy π	Round robin
BSR periodicity τ	1 ms
Transmission time interval TTI	1 ms
Carrier frequency f_D	2.63 GHz
Bandwidth B	5 MHz
Packet size L	150 Bytes [15]

IV. USE CASE I: POWER PARK

A. System Description

This case involves distributed control of N inverters connected to a common bus [9], as shown in Fig. 3.

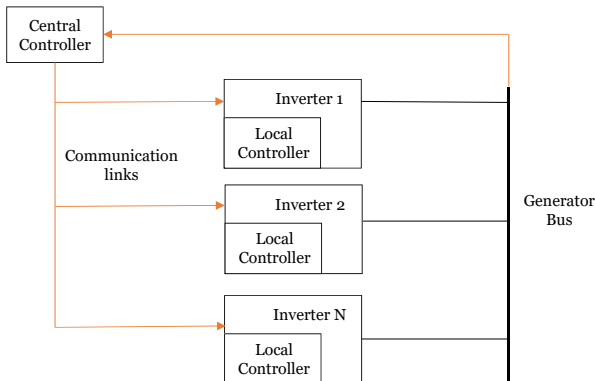


Fig. 3. Power park system model.

This case employs frequency partitioning, which divides the control tasks between the remote central controller and the distributed local controllers of each inverter. The concept of

frequency partitioning is shown in Fig. 4. This method reduces the required communication bandwidth between the remote central controller and the local controllers. The low frequency component of the control signal is provided by the central controller, while its high frequency component is generated by the local controllers. y^* denotes the reference signal for the central controller. The reference signal for the local controller is set to zero because disturbance rejection is desired at high frequency. LPF, and HPF represents the low pass and high pass filters.

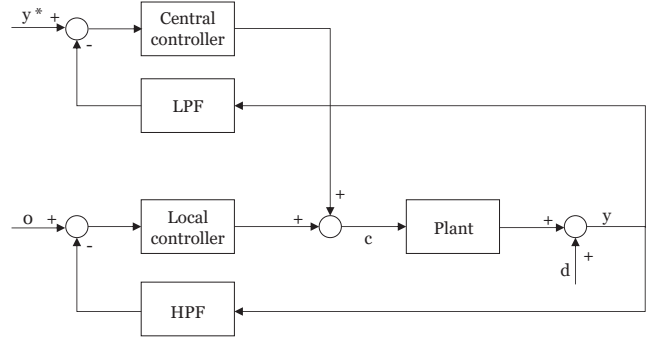


Fig. 4. Frequency partitioning for inverter control.

Our test system has three inverters, where each inverter contains an inner current control loop embedded within an outer voltage control loop. A 5G network is used to communicate the control signals from the central controller to the individual local controllers at each inverter. The inverters and loads are connected to the generator bus. Further details about this case can be found in [9].

B. Performance Evaluation

1) Set point change in voltage at the generator bus:

This case study evaluates voltage regulation at the common generator bus. The analysis is carried out in the dq -frame of reference. V_{oq} is set to zero and a step change is applied in V_{od} from 0.2 to 0.3 at $t = 0.07$ s. The system response is shown in Fig. 5. $V_{od-ideal}$ denotes the system simulation response under ideal conditions (5G channel is not used). V_{od-5G} denotes the system response with 5G communication channel (the low frequency control signal is communicated from the central controller to the individual local controllers). Table II shows the overshoot and settling time of the responses. The settling times for both the cases are around 0.01 s. There is, however, a change in overshoot from 1% to 10.3% in the presence of the 5G network.

TABLE II
OVERSHOOT AND SETTLING TIME FOR SET POINT CHANGE IN VOLTAGE AT THE GENERATOR BUS (POWER PARK CASE)

Case	Overshoot (%)	Settling Time (ms)
Ideal	1	11.1
5G	10.3	14.19

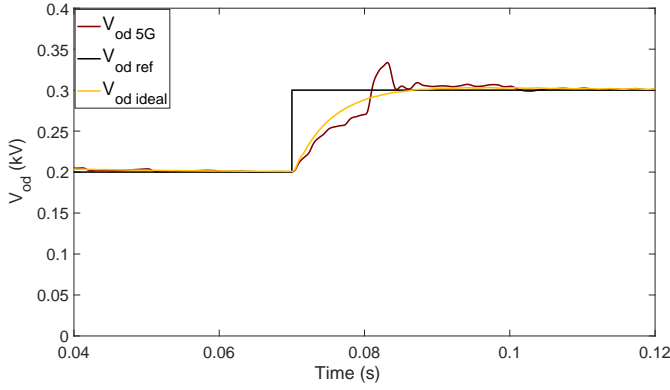


Fig. 5. Comparison of the system response (d -component of the voltage at the generator bus) to a step change in set-point with and without the 5G network.

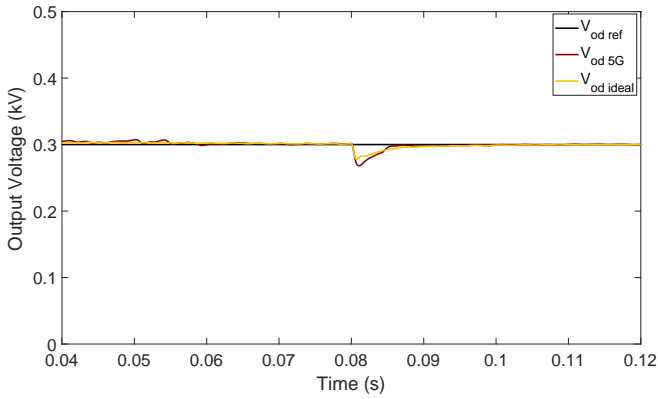
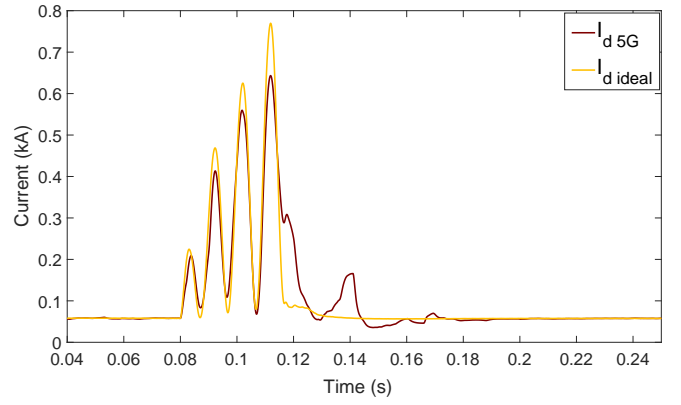


Fig. 6. Load switching of a three phase balanced RL load. Output voltage in dq frame (d -axis component).

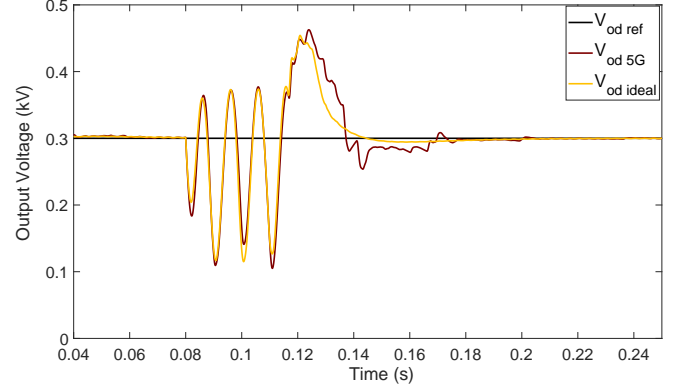
2) *Load switching*: The system with and without 5G communication network is subjected to a load switching condition. A three-phase balanced RL load is switched on and is connected to the system at $t = 0.08$ s. The transient response is shown in Fig. 6. This includes the d -axis component of the output voltage in dq -frame of reference. The results indicate similar transient performance for both cases. The transient lasts for around 5 ms in both the cases and the system does not lose its stability. The drop in voltage is around 0.01 V more with the 5G channel.

3) *Single-phase to ground fault at the generator bus*: A single-phase A-G fault is simulated at $t = 0.08$ s for 0.03 s at the generator bus. Fig. 7 shows the results. The system with 5G network does not lose its stability. It is able to continue tracking the reference value of the direct axis voltage at the generator bus after the fault is cleared. The transient lasts for about 0.065 s after the fault is cleared with 5G channel, while it lasts for around 0.028 s with ideal communication.

4) *Three-phase to ground fault at the generator bus*: A three-phase ABC-G fault is simulated at $t = 0.08$ s for 0.03 s at the generator bus. Fig. 8 shows the results. The system with 5G network does not lose its stability. It is able to continue tracking the reference value of the direct axis voltage at the generator bus after the three-phase to ground fault is cleared.



(a)



(b)

Fig. 7. Single-phase fault to ground (a) d -component of the output current of one of the inverters in dq -frame. (b) d -component of the output voltage at the generator bus in dq -frame.

The transient lasts for 0.13 s after the fault is cleared with 5G channel, while it lasts for 0.1 s with ideal communication.

V. USE CASE II: COORDINATED SET POINT MODULATION OF DERS

A. System Description

Set point modulation involves modulating the system set-point x_{sp} depending on the system response $x(t)$ [16]. Mathematically, this is given as

$$x'_{sp} = x_{sp} + me(t), \quad (2)$$

where x'_{sp} is the modulated set point, m is a design parameter, and $e(t)$ is the tracking error that measures the deviation of the system response from the set point.

$$e(t) = x_{sp} - x(t). \quad (3)$$

For better dynamic response, the tracking error $e(t)$ is replaced by the predictive dynamic behaviour of the tracking error. That is,

$$x'_{sp} = x_{sp} + m\hat{e}_{pred}(t). \quad (4)$$

There are different methods that can be used to obtain $\hat{e}_{pred}(t)$, but this case uses a linear expression.

The above equations are for a single DER. Another level of control can be added with the help of communication

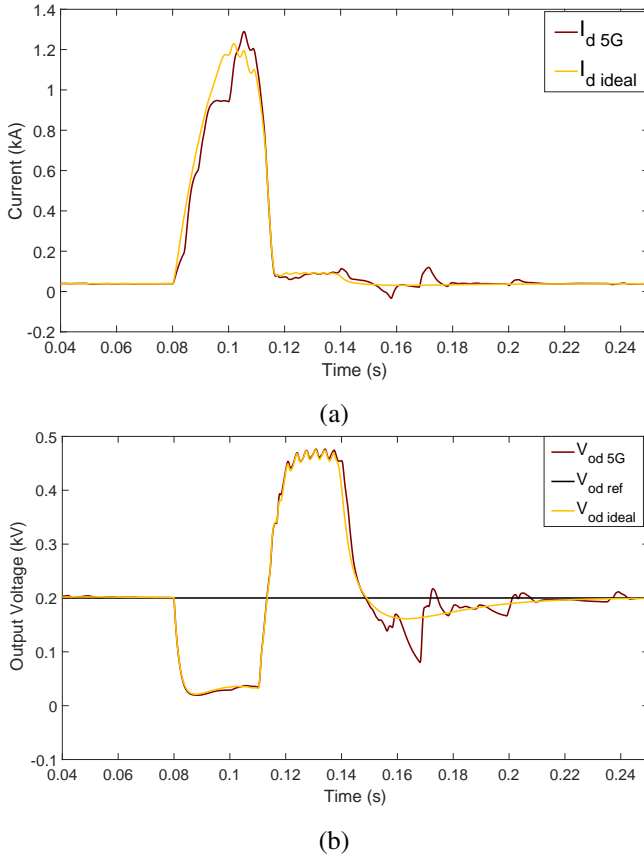


Fig. 8. Three-phase fault to ground (a) d -component of the output current of one of the inverters in dq -frame. (b) d -component of the output voltage at the generator bus in dq -frame.

between different DERs known as coordinated set point modulation [10]. Consider N devices connected at the PCC that are capable of exchanging information over a communication channel. The devices connected through a communication link exchange information about their respective predictive tracking errors. The existing equation for a single DER can be modified to represent the system response for the i th DER as

$$x'_{i_{sp}} = x_{i_{sp}} + m_i \hat{e}_{i_{pred}}(t) \quad (5)$$

The secondary level of control $u(t)$ can then be defined as:

$$u(t) = m_i \sum_{j=1, j \neq i}^N a_{ij} \hat{e}_{j_{pred}}(t) \quad (6)$$

where a_{ij} denotes a communication link between DER i and DER j . Hence the control equation can be represented by

$$x'_{i_{sp}} = x_{i_{sp}} + m_i \hat{e}_{i_{pred}}(t) + m_i \sum_{j=1, j \neq i}^N a_{ij} \hat{e}_{j_{pred}}(t) \quad (7)$$

Further details about this concept can be found in [10].

B. Performance Evaluation

Fig. 9 shows the three devices (DERs) that interact with each other using coordinated set-point modulation.

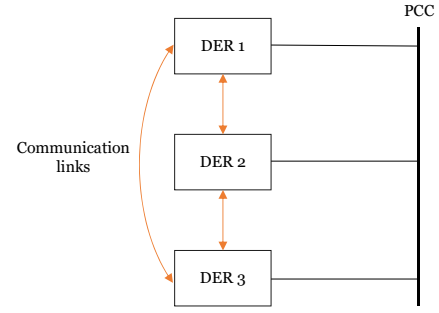


Fig. 9. System model of coordinated set point modulation of DERs.

1) *Staggered set point change*: A staggered set point change is applied to the individual devices (step change in reference point from 0 to 1 at $t = 0.5$ s for DER 1, at $t = 1$ s for DER 2 and at $t = 1.5$ s for DER 3). These set points can represent any electrical quantity that needs control (voltage, real power or reactive power). The combined system response at the PCC, under ideal simulation conditions (no 5G communication involved) and in the presence of a 5G network, is shown in Fig. 10. Table III shows the overshoot and the settling time of the system response under the two conditions. The settling time increases by 172 ms in the presence of a 5G network and the overshoot is twice the ideal simulation condition. However, the DERs are able to track the set point changes successfully with 5G communication.

2) *Simultaneous set point change*: A simultaneous set point change is applied to all the devices (step change in reference point from 0 to 1 at $t = 0.5$ s). The set point is brought back to 0 for all the devices at $t = 2$ s. The combined system response at the PCC, under ideal simulation conditions and in the presence of a 5G network, is shown in Fig. 11. Table III shows the overshoot and the settling time of the system response under the two conditions. The settling time increases by 84 ms in the presence of a 5G network and the overshoot is higher by 11.4%. However, the set points are tracked successfully without loss in stability.

3) *Communication failure in one of the devices*: The system performance is evaluated when one of the devices is incapable of communicating its state to the other two devices. The response is shown in Fig. 12. The response is also compared with the scenario in which all the devices can communicate without any hindrance. Although there is an increase in overshoot and settling time, the system is able to track the set points owing to the control algorithm used. This can be seen from the first two terms in (7). These terms do not depend on the states of the other devices, thus contributing towards set point tracking in the absence of information from one device.

- [11] “3GPP TS 38.306. User Equipment (UE) radio access capabilities. version 15.3.0 Rel 15.”
- [12] “3GPP TS 38.214. Physical layer procedures for data version. 15.3.0 Rel 15.”
- [13] R. Dilli, “Analysis of 5G Wireless Systems in FR1 and FR2 Frequency Bands,” in *2020 2nd International Conference on Innovative Mechanisms for Industry Applications (ICIMIA)*, Mar. 2020, pp. 767–772.
- [14] “NR Scheduling Performance Evaluation - MATLAB & Simulink,” <https://www.mathworks.com/help/5g/ug/nr-tdd-symbol-based-scheduling-performance-evaluation.html>, (Accessed on 01/11/2021).
- [15] “Ericsson Mobility Report November 2016,” <https://www.ericsson.com/en/mobility-report/reports>, (Accessed on 12/06/2020).
- [16] A. Mehrizi-Sani and R. Iravani, “Online set point modulation to enhance microgrid dynamic response: Theoretical foundation,” *IEEE Transactions on Power Systems*, vol. 27, no. 4, pp. 2167–2174, Nov. 2012.